

# Electrochemical Corrosion Behavior of Arc Sprayed Zn and Zn15Al Coatings in Simulated Salina Soil and Neutral Meadow Soil Solutions

LIN Bilan<sup>1</sup>, LU Xinying<sup>1</sup>, LI Long<sup>2</sup>

(1. Graduate School at Shenzhen, Tsinghua University, Shenzhen 518055, China; 2. Guangdong Sanhe Pipe-pile Co. Ltd., Zhongshan 518424, China)

**Abstract:** Arc sprayed Zn and Zn15Al coatings were chosen to protect the metal ends of prestressed high-strength concrete (PHC) pipe piles against corrosion of salina soil in northern China and neutral meadow soil in northeast China. The corrosion behavior of the coated Q235 steel samples in two simulated soil solutions were investigated by potentiodynamic polarization and electrochemical impedance spectroscopy (EIS) methods. The experimental results show that the corrosion of the matrix Q235 steel in both simulated solutions is remarkably inhibited by Zn and Zn15Al coatings. The corrosion products on Zn and Zn15Al are thick, compact, firm and protective. The corrosion current density  $i_{\text{corr}}$  of both Zn and Zn15Al-coated samples is decreased evidently with corrosion time, and the charge transfer resistance  $R_{\text{ct}}$  is increased greatly. The corrosion resistance indexes of Zn and Zn15Al in simulated neutral meadow soil solution are more outstanding than those in salina soil. The corrosion resistance of Zn15Al in salina soil is slightly superior to that of Zn. When the sprayed coatings are sealed with epoxy resin, the corrosion resistance of the coatings is further enhanced markedly.

**Key words:** arc spray; coating; soil; corrosion; electrochemical

## 1 Introduction

PHC pipe piles are increasingly to be used in some aggressive areas of Northern and Northeast China, which have been originated and widely used in Southern China. With the demanding durability requirements about the engineering structures<sup>[1,2]</sup>, the durability of PHC pipe piles should be clarified as the anticorrosion behavior of the pile body and the metal ends. The durability of the concrete pile body has been investigated and the improved measures were put forward<sup>[3]</sup>. However, there are few attentions being paid to the corrosion behavior of the metal ends. The metal ends of PHC pipe piles consist of apron, end plate and steel bar, which the materials are different. In corrosive soil, various corrosion such as chemical, electrochemical and galvanic corrosion will occur<sup>[4,5]</sup>. Lin *et al*<sup>[6]</sup> has found that the corrosion resistance of the steel bar is inferior to that of the end plate; the corrosion resistance grade of the steel bar in saline soil

is poor; and steel bar is anodic and end plate is cathodic when they were coupled in soils. The durability of PHC pipe piles would be impaired, and the safety of the engineering structures might thus be affected.

Arc sprayed metal coatings have been widely applied to the corrosion protection of the metal structures<sup>[7-11]</sup>. Zinc, aluminum and zinc-aluminum alloy coatings can be acted as both physical barriers and sacrificial anodes, and the corrosion products are protective. Recent reports about the corrosion behavior of the sprayed metal coatings in marine environment could be found<sup>[12-15]</sup>, but that in aggressive soils is scarcely<sup>[16]</sup>.

The soils in northern and northeast China are characterized separately as salina and neutral meadow soil. In this paper, arc sprayed Zn and Zn15Al coatings were used to protect the metal ends of PHC pipe piles against the corrosion of these two soils. The corrosion behavior of the coated Q235 steel in simulated soil solutions was studied.

## 2 Experimental

The matrix material was cold-rolled Q235 steel. Zn and Zn15Al wires ( $\phi$  2 mm) were as the sprayed material. The purity of Zn is 99.99wt%. Zn15Al alloy contains 15wt% Al and balanced Zn.

The arc spraying parameters are as follows: spray

voltage 28 V, spray current 200 A, spray distance 200 mm and air pressure 0.65 MPa. The thickness of the sprayed coatings is about 160 μm.

The simulated solutions of salina soil in northern China and neutral meadow soil in northeast china were prepared on the basis of the physicochemical properties of salina soil in “Code for Investigation of Geotechnical Engineering (GB50021-2008)” and neutral meadow soil in shenyang national soil corrosion test station, respectively. The chemical composition and pH value of them are listed in Table 1.

**Table 1 Chemical compositions and pH values of two simulated soil solutions**

Soil type	Chemical compositions/(g · L <sup>-1</sup> )			pH
	NaCl	Na <sub>2</sub> SO <sub>4</sub>	NaHCO <sub>3</sub>	
Salina	1.810	17.74	-	8.6
Neutral meadow	0.028	0.190	0.110	7.4

Potentiodynamic polarization and EIS measurements were carried out using electrochemical workstation (Model: CS360) with a conventional three-electrode cell system. A Saturated Calomel Electrode (SCE) was used as a reference electrode, and a platinum electrode was served as an auxiliary electrode. The exposed area of the working electrode was 1.0 cm<sup>2</sup>. The scan rate for polarization was 1 mV/s. EIS measurements were performed at corrosion potential in a frequency range between 100 kHz and 0.01 Hz with a potential sine signal of 10 mV. The EIS diagrams were analyzed and fitted using a Zview software.

The sample coated with pure Zn was denoted as Zn, and that with Zn15Al was denoted as Zn15Al.

### 3 Results and Discussion

#### 3.1 Potentiodynamic polarization analysis

**Table 2 E<sub>corr</sub> and i<sub>corr</sub> of Zn and Zn15Al immersed in two simulated soil solutions**

Sample	Salina soil		Sample	Neutral meadow soil	
	E <sub>corr</sub> /(mV vs SCE)	I <sub>corr</sub> /(μA · cm <sup>-2</sup> )		E <sub>corr</sub> /(mV vs SCE)	I <sub>corr</sub> /(μA · cm <sup>-2</sup> )
Zn	-1257.5	23.1	Zn	-1199.2	2.33
Zn15Al	-1351.4	14.6	Zn15Al	-1235.7	2.43

**Table 3 E<sub>corr</sub> and i<sub>corr</sub> of Zn and Zn15Al immersed in two simulated soil solutions for different time**

Sample	Time	Salina soil		Sample	Time	Neutral meadow soil	
		E <sub>corr</sub> /(mV vs SCE)	I <sub>corr</sub> /(μA · cm <sup>-2</sup> )			E <sub>corr</sub> /(mV vs SCE)	I <sub>corr</sub> /(μA · cm <sup>-2</sup> )
Zn	30 min	-1257.5	23.1	Zn	30 min	-1199.2	2.33
	30 d	-1086.5	5.09		30 d	-936.0	1.06
	50 d	-	-		50 d	-774.6	0.38
	70 d	-1061.6	0.46		70 d	-855.6	0.12
	155 d	-1013.8	0.87		155 d	-664.4	0.10
Zn15Al	30 min	-1351.4	14.6	Zn15Al	30 min	-1235.7	2.43
	30 d	-1073.6	3.99		30 d	-958.1	2.30
	50 d	-1065.8	1.14		50 d	-930.9	0.87
	70 d	-1064.8	0.82		70 d	-925.9	0.15
	155 d	-1088.5	1.08		155 d	-754.5	0.13

Only white rusts were observed when Zn and Zn15Al were immersed in simulated solutions of salina soil and neutral meadow soil for 200 days. The corrosion products are not flaked off after intense vibration in solution. And the exposed surface of the coatings is insulated to the external conducting wire which was welded on back of the sample and sealed by epoxy resin. The corrosion products on Zn and Zn15Al are thick, firm and insulated, which thus can effectively inhibit the corrosion of the matrix Q235 steel.

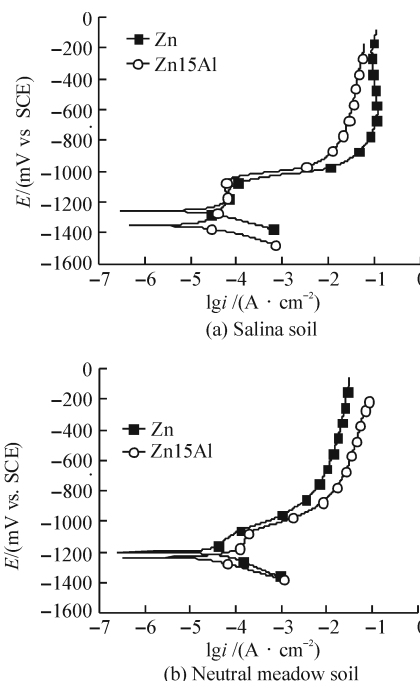


Fig.1 Polarization curves of Zn and Zn15Al in two simulated solutions

Fig.1 shows the polarization curves of Zn and Zn15Al immersed in two simulated soil solutions, and the corresponding corrosion potential E<sub>corr</sub> and

corrosion current density  $i_{\text{corr}}$  are listed in Table 2.

As shown in Fig.1, the polarization curves of Zn and Zn15Al in two simulated soil solutions is similar. The cathodic process is controlled by activation polarization, but the cathodic branch of Zn15Al is at the left side of Zn. The change of the anodic process is as following: a passivation region near  $E_{\text{corr}}$ , a quick increase of  $i$  with  $E$ , another passivation region when  $E$  is higher than about  $-800$  mV. The first passivation region in salina soil is larger than that in neutral meadow soil, and that of Zn15Al is slightly greater than that of Zn in the same solution. Compared with Zn, the anodic branch of Zn15Al in salina soil is appreciably left-shifted, while in neutral meadow soil it is slightly right-shifted.

In Table 2,  $E_{\text{corr}}$  of Zn and Zn15Al in salina soil is more negative than that in neutral meadow soil. This may be due to that  $E_{\text{corr}}$  is related to ionic activity and pH of solution<sup>[17]</sup>. And  $i_{\text{corr}}$  of Zn and Zn15Al in neutral meadow soil is quite smaller than that in salina soil.

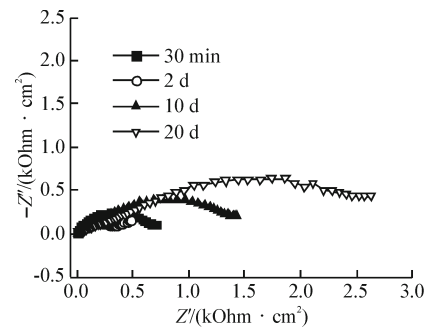
Table 3 shows  $E_{\text{corr}}$  and  $i_{\text{corr}}$  of Zn and Zn15Al immersed in two simulated solutions for different time. With an increase in corrosion time,  $E_{\text{corr}}$  and  $i_{\text{corr}}$  of Zn and Zn15Al are increased differently,  $i_{\text{corr}}$  of them at 155 days is more than one order of magnitude smaller than that at 30 min, due to the protective corrosion products.  $i_{\text{corr}}$  of them in neutral meadow soil is markedly smaller than that in salina soil, which can be attributed to the fewer content of the corrosive ions of chloride and sulfate in the former soil.  $i_{\text{corr}}$  of Zn in neutral meadow soil is slightly smaller than that of Zn15Al. In salina soil,  $i_{\text{corr}}$  of Zn in the initial corrosion stage is larger than that of Zn15Al, but in the middle and later corrosion periods the former is appreciably smaller than that of Zn15Al.

### 3.2 EIS analysis

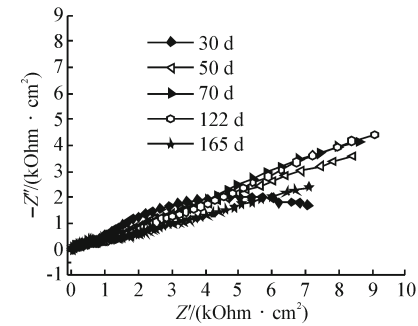
Fig.2 shows the Nyquist diagrams of Zn and Zn15Al immersed in simulated salina soil solution for different time (The change law of them in neutral meadow soil solution is similar). Prolonging the corrosion time, the size of the impedance diagrams is increased greatly, indicating a large increase of the impedance value of Zn and Zn15Al.

As shown in Fig.2, these EIS diagrams are composed of two time constants which are corresponding to high frequency capacitive loop (HFCL) and low frequency capacitive loop (LFCL). In the case of a shorter corrosion time, HFCL can be attributed to the capacitance and the pore resistance of the arc sprayed coatings. For a longer time, HFCL can be ascribed to the capacitance and the resistance of the corrosion products. LFCL can be attributed to the capacitance of the electric double layer of the solution/substrate interface and the charger transfer resistance<sup>[14,18]</sup>.

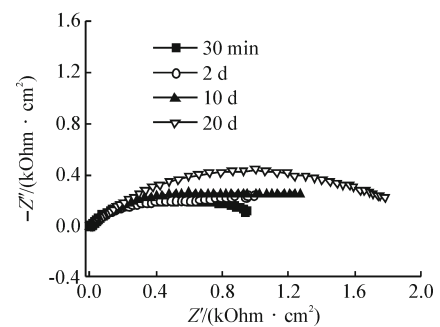
The EIS diagrams in Fig.2 can be described by



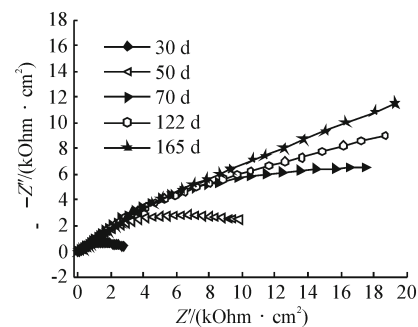
(a.) Zn for a shorter time



(a.) Zn for a longer time



(b.) Zn15Al for a shorter time



(b.) Zn15Al for a longer time

Fig.2 Nyquist diagrams of Zn and Zn15Al immersed in simulated salina soil solution for different time

Fig.3.  $R_s$  is the solution resistance, CPEr is the HFCL capacitance and  $R_r$  is the pore resistance; CPEdl is the LFCL capacitance of the electric double layer and  $R_{ct}$  is the charge transfer resistance.

Comparing with the pure capacitance, the frequency response characteristics of the capacitance in practical electrochemical system is deviated which is manifested as the depression of the semicircle in Nyquist diagram<sup>[19-21]</sup>. And a constant-phase element of CPE is used to characterize the practical capacitance

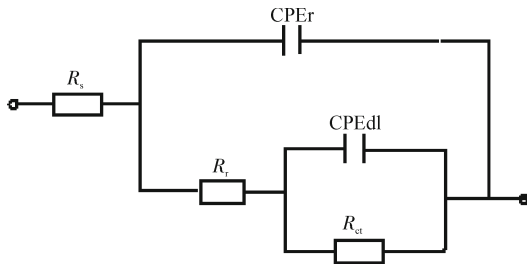


Fig.3 Equivalent circuit model

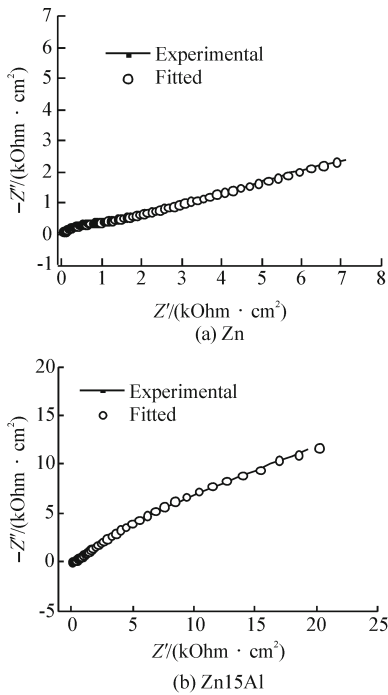


Fig.4 Comparison of the experimental and fitted curves

of the electric double layer. CPE has an impedance dispersion relation of  $Q=1/Y_0(j\omega)^n$ , where,  $n$  can be expressed as  $n=1-2\alpha/180$ ,  $\alpha$  is the depression angle of the semicircle. If  $n=1, 0$  or  $-1$ , CPE represents a capacitance ( $C$ ), a resistance ( $R$ ) or an inductance

( $L$ ), respectively. When  $0 < n < 1$ , CPE is denoted as the dispersion effect of the capacitance of the electric double layer.

Fig.4 shows the experimental and fitted curves of Zn and Zn15Al immersion in simulated salina soil solution for 165 days. It is found that the fitted curves follow well with the experimental curves, and the fitting error is less than 10%. Thus the proposed equivalent circuit model is feasible.

Table 4 lists the EIS fitted parameters of  $Y_0$ -CPEdl,  $n$ -CPEdl and  $R_{ct}$  at LFCL of Zn and Zn15Al.  $n$ -CPEdl is in the range of  $0 < n$ -CPEdl  $< 1$ . Benedetti *et al*<sup>[22]</sup> found that the smoother and more clear the electrode surface is, the larger the  $n$  value is. The surface of the sprayed coatings is coarse<sup>[13,15]</sup>, and the species and quantity of the corrosion products adsorbed on the micro-regions of the electric double layer are different.

As shown in Table 4,  $Y_0$ -CPEdl of both Zn and Zn15Al in salina soil and Zn15Al in neutral meadow is increased with corrosion time from 30 min to 2 days but decreases gradually for a longer corrosion. Because the capacitance value is proportional to the dielectric constant and the surface area, and it is inverse proportional to the distance of the two layers<sup>[23]</sup>. When the surface of the sprayed coatings is covered with the corrosion products, the dielectric constant will be decreased<sup>[19]</sup>. The more compact the corrosion products' layer is, the smaller the surface area of the capacitance is. The thicker the layer of the corrosion products is, the longer the distance of the two layers is. The increase of  $Y_0$ -CPEdl in the initial stage of corrosion may be due to the quicker dissolution of Zn or Zn15Al than the formation of the corrosion products. The decrease of  $Y_0$ -CPEdl value can be attributed to the slower dissolution of the coatings, and the gradual formation, the stable existence, the densification and

Table 4 EIS parameters of  $Y_0$ -CPEdl,  $n$ -CPEdl and  $R_{ct}$  of Zn and Zn15Al immersed in two simulated soil solutions for different time

Sample	Corrosion time	Salina soil			Sample	Corrosion time	Neutral meadow soil		
		$Y_0$ -CPEdl / $(\Omega^{-1} \cdot \text{cm}^{-2} \cdot \text{s}^{-n})$	$n$ -CPEdl	$R_{ct}$ / $(\Omega \cdot \text{cm}^2)$			$Y_0$ -CPEdl / $(\Omega^{-1} \cdot \text{cm}^{-2} \cdot \text{s}^{-n})$	$n$ -CPEdl	$R_{ct}$ / $(\Omega \cdot \text{cm}^2)$
Zn	30 min	$5.864 \times 10^{-4}$	0.783	700	Zn	30 min	$4.059 \times 10^{-4}$	0.576	1529
	2 d	$15.01 \times 10^{-4}$	0.514	489		2 d	$1.214 \times 10^{-4}$	0.453	3651
	10 d	$5.046 \times 10^{-4}$	0.473	1492		10 d	$0.3982 \times 10^{-4}$	0.313	55977
	20 d	$3.591 \times 10^{-4}$	0.349	2826		20 d	$0.2439 \times 10^{-4}$	0.275	87880
	30 d	$1.967 \times 10^{-4}$	0.489	10068		30 d	$0.1861 \times 10^{-4}$	0.293	97617
	50 d	-	-	-		50 d	$0.1410 \times 10^{-4}$	0.322	188170
	70 d	$2.354 \times 10^{-4}$	0.289	16560		70 d	$0.1169 \times 10^{-4}$	0.316	240050
	120 d	$2.529 \times 10^{-4}$	0.309	25322		120 d	$0.1212 \times 10^{-4}$	0.314	277590
	165 d	$2.558 \times 10^{-4}$	0.219	22660		165 d	$0.09192 \times 10^{-4}$	0.332	331500
	Zn15Al	30 min	$2.629 \times 10^{-4}$	0.655		842	Zn15Al	30 min	$1.000 \times 10^{-4}$
2 d		$3.765 \times 10^{-4}$	0.636	844	2 d	$1.514 \times 10^{-4}$		0.592	2555
10 d		$3.496 \times 10^{-4}$	0.537	1260	10 d	$0.8172 \times 10^{-4}$		0.556	4921
20 d		$1.976 \times 10^{-4}$	0.550	1861	20 d	$0.6125 \times 10^{-4}$		0.534	12056
30 d		$1.608 \times 10^{-4}$	0.534	2979	30 d	$0.4473 \times 10^{-4}$		0.520	19380
50 d		$1.180 \times 10^{-4}$	0.536	12861	50 d	$0.3629 \times 10^{-4}$		0.485	57852
70 d		$1.050 \times 10^{-4}$	0.534	29458	70 d	$0.2815 \times 10^{-4}$		0.487	96374
120 d		$1.039 \times 10^{-4}$	0.538	38157	120 d	$0.2365 \times 10^{-4}$		0.505	126040
165 d		$1.036 \times 10^{-4}$	0.492	56779	165 d	$0.1834 \times 10^{-4}$		0.546	169030

the thickening of the corrosion products.

$R_{ct}$  of Zn and Zn15Al in two simulated solutions is markedly increased with corrosion time, as shown in Table 4.  $R_{ct}$  represents the resistance of the charge transfer. The thicker and more compact the corrosion products are, the more difficult the charge transfer is.

As shown in Table 4,  $Y_0$ -CPEdl of Zn and Zn15Al in neutral meadow soil is very smaller than that in salina soil, and  $R_{ct}$  in neutral meadow soil is significantly larger than that in salina soil.  $n$ -CPEdl of Zn in two simulated solutions is smaller than that of Zn15Al. In the middle and later stages of corrosion, the corrosion resistance indexes of Zn15Al in salina soil are more outstanding than those of Zn, while in neutral meadow soil the former is worse than the latter. This is in good agreement with the result of the potentiodynamic polarization.

## 4 Conclusion

The corrosion of the matrix Q235 steel in simulated solutions of salina soil in Northern China and neutral meadow soil in Northeast China is effectively inhibited by arc sprayed Zn and Zn15Al coatings. With an increase in corrosion time,  $i_{corr}$  is decreased greatly, and  $R_{ct}$  is increased. In the later corrosion stage,  $i_{corr}$  is reduced for more than one order of magnitude, and  $R_{ct}$  is increased for about one to two orders of magnitude. The corrosion resistance indexes of Zn and Zn15Al in simulated neutral meadow soil solution are more outstanding than those in simulated salina soil solution. The corrosion resistance of Zn15Al in simulated salina soil solution is appreciably better than those of Zn, while in simulated neutral meadow soil solution that of Zn is slightly superior to that of Zn15Al.

## References

- [1] Fisher A K, Bullen F, Beal D. The Durability of Cellulose Fibre Reinforced Concrete Pipes in Sewage Applications [J]. *Cem. Concr. Res.*, 2001, 31(4): 543-553
- [2] Miyata Y, Nakano H, Abe M, et al. Effectiveness of Polyethylene Coating for Steel Pipe Piles [J]. *Mater. Perform.*, 2006, 45(12): 24-27
- [3] Han Q W, Wei Y L. Low Durability of PHC Pipe Piles [N]. *Guangdong Jianshe Newspaper*, 2006-12-29-B03
- [4] Berger D M. Electrochemical and Galvanic Corrosion of Coated Steel Surfaces [J]. *Chem. Eng. (New York)*, 1982, 89: 109-112
- [5] Du C W, Li X G, Liang P, et al. Effects of Microstructure on Corrosion of X70 Pipe Steel in an Alkaline Soil [J]. *J. Mater. Eng. Perform.*, 2009, 18(2): 216-220
- [6] Lin B L, Lu X Y, Li L. Corrosion Behaviors of Metal End of PHC Pipe Pile in Simulated Soil Solutions [J]. *J. Central South Univ. (Sci. Technol.)*, 2011, 42(2): 434-440
- [7] Vourlias G, Pistofidis N, Stergioudis G. Ability of Metallic Coatings to Protect Low Carbon Steels from Aqueous Corrosion [J]. *Corros. Eng. Sci. Technol.*, 2008, 43(2): 163-172
- [8] Papavinasam S, Attard M, Arseneult B, et al. State-of-the-art of Thermal Spray Coatings for Corrosion Protection [J]. *Corros. Rev.*, 2008, 26(2-3): 105-146
- [9] Hou B R, Zhang J, Duan J Z, et al. Corrosion of Thermally Sprayed Zinc and Aluminium Coatings in Simulated Splash and Tidal Zone Conditions [J]. *Corros. Eng. Sci. Technol.*, 2003, 38(2): 157-160
- [10] Tobe S. A Review on Protection from Corrosion, Oxidation and Hot Corrosion by Thermal Spray Coatings.// ASM Thermal Spray Society, German Welding Society, and High Temperature Society of Japan. Nice: *ASM International*, 1998: 3-11
- [11] Lee S H, Lee H S, Kyung J W, et al. Anti-Corrosion Performance of Zn-Al Thermal Metal Spraying Method Using Steel Structures [J]. *Key Eng. Mater. Adv. Fract. Damage Mech. VI*, 2007, 348-349: 453-456
- [12] Liu Y, Zhu Z X, Chen Y X, et al. Electrochemical Corrosion Behavior of Arc Sprayed Zn-Al Coatings [J]. *Trans. Nonferrous Met. Soc. China*, 2004, 14(S1): 443-445
- [13] Chaliampalias D, Vourlias G, Pistofidis N, et al. A Morphological and Microstructural Study of Flame-Sprayed Zinc Coatings on Low-Alloyed Steels as a Contribution to Explaining their Corrosion Resistance [J]. *Phys. Status Solidi. (A) Appl. Mater.*, 2008, 205(7): 1566-1571
- [14] Tsuyoshi M, Kazuo F, Yasuyuki T, et al. Corrosion Rate and Corrosion Behavior of Al-2%Zn Alloy Spray Coating in Sodium Chloride Solution at Low Temperature [J]. *Corros. Eng.*, 2005, 54(11): 520-525
- [15] Kuroda S, Kawakita J, Takemoto M. An 18-year Exposure Test of Thermal-Sprayed Zn, Al, and Zn-Al Coatings in Marine Environment [J]. *Corrosion*, 2006, 62(7): 635-647
- [16] Lin B L, Lu X Y, Li L. Corrosion Behaviors of Arc Spraying Single and Double Layer Coatings in Simulated Dagang Soil Solution [J]. *Trans. Nonferrous Met. Soc. China*, 2009, 19(6): 1 556-1 561
- [17] Yang X Z, Yang W. *Electrochemical Thermodynamics of Metallic Corrosion: Potential-pH Diagrams and their Applications* [M]. Beijing: Chemical Industry Press, 1991: 21-86
- [18] Cachet C, Ganne F, Joiret S, et al. EIS Investigation of Zinc Dissolution in Aerated Sulphate Medium. Part II: Zinc Coatings [J]. *Electrochim. Acta*, 2002, 47(21): 3409-3422
- [19] Cao C N, Zhang J Q. *Introduction to Electrochemical Impedance Spectroscopy* [M]. Beijing: Science Press, 2002: 143-189
- [20] Weng D, Jokiel P, Uebleis A, et al. Corrosion and Characteristics of Zinc and Manganese Phosphate Coatings [J]. *Surf. Coat. Technol.*, 1997, 88(1-3): 147-156
- [21] Tang N, Ooij W J, Gorecki G. Comparative EIS Study of Pretreatment Performance in Coated Metals [J]. *Prog. Org. Coat.*, 1997, 30(4): 255-263
- [22] Benedetti A V, Sumodjo P T A, Nobe K, et al. Electrochemical Studies of Copper, Copper-Aluminium and Copper-Aluminium-Silver Alloys: Impedance Results in 0.5 M NaCl [J]. *Electrochim. Acta*, 1995, 40(16): 2657-2668
- [23] Yao J M. *College Physics (II)* [M]. Beijing: Beijing Institute of Technology Press, 2008: 317-322